Molecular & Biochemical Parasitology 173 (2010) 132–141

Contents lists available at ScienceDirect

Molecular & Biochemical Parasitology

Identification, cloning and characterization of an aldo-keto reductase from *Trypanosoma cruzi* with quinone oxido-reductase activity☆

Patricia A. Garavaglia[a], Joaquín J.B. Cannata[b,c], Andrés M. Ruiz[a], Dante Maugeri[c], Rosario Duran[d], Mónica Galleano[e], Gabriela A. García[a,*]

[a] *Instituto Nacional de Parasitología "Dr. Mario Fatala Chaben" - A.N.L.I.S. "Dr. Carlos G. Malbrán", Buenos Aires 1063, Argentina*
[b] *CEFYBO, Facultad de Medicina, Universidad de Buenos Aires, Buenos Aires 1113, Argentina*
[c] *Instituto de Investigaciones Biotecnológicas (IIB–INTECH), Universidad Nacional de General San Martín - CONICET, San Martín 1650, Buenos Aires, Argentina*
[d] *Instituto de Investigaciones Biológicas "Clemente Estable", Instituto Pasteur de Montevideo, Montevideo 11600, Uruguay*
[e] *Fisicoquímica - PRALIB, Facultad de Farmacia y Bioquímica, Universidad de Buenos Aires - CONICET, Buenos Aires 1113, Argentina*

ARTICLE INFO

Article history:
Received 1 December 2009
Received in revised form 24 May 2010
Accepted 25 May 2010
Available online 2 June 2010

Keywords:
Trypanosoma cruzi
Chagas' disease
Aldo-keto reductase
Drug metabolism
Quinone
Free radicals

ABSTRACT

Drugs currently used for treatment of *Trypanosoma cruzi* infection, the ethiological agent of Chagas' disease, have shown side effects and variable efficiency. With the aim to describe parasite enzymes involved in the mechanisms of action of trypanocidal drugs and since it has been reported that reductases are crucial in their metabolism, we attempted to identify novel NADPH-dependent oxido-reductases from *T. cruzi*. The percolation of a soluble fraction of epimastigote lysates through a Cibacron Blue-Sepharose column followed by elution by NADPH yielded a predominant protein with an apparent molecular weight of 32 kDa. This protein was identified by MALDI-TOF as an aldo-keto reductase (AKR) and hence denominated *Tc*AKR. *Tc*AKR was mainly localized in the cytosol and was also present in trypomastigote and amastigote lysates. The recombinant *Tc*AKR (rec*Tc*AKR) showed NADPH-dependent reductase activity with the AKR substrates 4-nitrobenzaldehyde and 2-dihydroxyacetone. The saturation curves for both substrates were consistent with the Michaelis–Menten model. We also tested whether rec*Tc*AKR may reduce naphthoquinones (NQ), since many of these compounds have displayed important trypanocidal activity. rec*Tc*AKR reduced *o*-NQ (1,2-naphthoquinone, 9,10-phenanthrenquinone and β-lapachone) with concomitant generation of free radicals but did not exhibit affinity for *p*-NQ (5-hydroxy-1,4-naphthoquinone, 2-hydroxy-1,4-naphthoquinone, α-lapachone and menadione). The substrate saturation curve with *o*-NQ fitted to a sigmoidal curve, suggesting that rec*Tc*AKR presents a cooperative behavior. In addition, three peaks assigned to monomers, dimers and tetramers were obtained when rec*Tc*AKR was submitted to a Superose 12 gel chromatography column. *Tc*AKR is the first member of the AKR family described in *T. cruzi*. Our results indicate that this enzyme may participate in the mechanisms of action of trypanocidal drugs.

1. Introduction

Chagas' disease, which is caused by the parasitic protozoan *Trypanosoma cruzi*, affects approximately 18 million people in Latin America, where the disease is a major public health and economic problem. *T. cruzi* is transmitted to mammalian hosts by blood-sucking triatomine bugs and infection results in a life-threatening, acute, and/or chronic disease with several complications [1,2]. The control of this endemia is worsened by several factors, such as the lack of a vaccine and the limited success of current antichagasic drugs, nifurtimox and benznidazole, due to their undesirable side effects, the variable efficacy in the chronic phase of the infection, and the emergence of parasite resistance [3].

T. cruzi has a limited ability to deal with reactive oxygen species (ROS) since, at variance with most eukaryotes, the parasite is devoid of catalase and glutathione reductase. However, it possesses

Abbreviations: AKR, aldo-keto reductase; BN-PAGE, blue native polyacrylamide gel electrophoresis; 2-DHA, 2-dihydroxyacetone; DMPO, 5,5′-dimethyl-1-pyrroline N-oxide; ESR, electron spin resonance; 4-NBA, 4-nitrobenzaldehyde; NQ, naphthoquinone; 1,2-NQ, 1,2-naphthoquinone; 2H-1,4-NQ, 2-hydroxy-1,4-naphthoquinone; 5H-1,4-NQ, 5-hydroxy-1,4-naphthoquinone; MALDI-TOF-MS, matrix assisted laser desorption/ionization time of flight mass spectrometry; PGFS, prostaglandin $F_{2\alpha}$ synthase; 9,10-PQ, 9,10-phenanthrenquinone; QOR, quinone oxido-reductase; rec*Tc*AKR, recombinant *Trypanosoma cruzi* aldo-keto reductase; ROS, reactive oxygen species; SOD, superoxide dismutase; *Tc*AKR, *Trypanosoma cruzi* aldo-keto reductase; *Tc*OYE, *Trypanosoma cruzi* old yellow enzyme.

☆ *Note:* The nucleotide sequence of *Trypanosoma cruzi Tc*AKR reported in this paper is available in the GenBank database under the accession number EU558869.

* Corresponding author. Tel.: +54 11 4331 2330; fax: +54 11 4331 7142.
E-mail address: gaandgarcia@yahoo.com (G.A. García).

0166-6851/$ – see front matter © 2010 Elsevier B.V. All rights reserved.
doi:10.1016/j.molbiopara.2010.05.019

an analogous redox system centered upon the trypanosomatid-specific thiol trypanothione [4–7]. ROS may be generated by a number of mechanisms, including drug metabolism. It has been proposed that trypanocidal drugs such as nitroheterocycles and naphthoquinones (NQ), are reduced by parasite reductases to form drug anion radicals which, under aerobic conditions, give rise to the formation of toxic oxygen metabolites [8,9]. Moreover, it has been documented that these drugs interact with flavoenzymes from *T. cruzi*, such as trypanothione reductase, lipoamide dehydrogenase and old yellow enzyme (*Tc*OYE), generating free radical production through redox cycling [10–12,3]. However, several lines of evidence suggest that other redox enzymes from the parasite are responsible for the first reduction step of these compounds [12]. As the identification and functional analysis of parasite enzymes involved in the oxidative defense system may be of importance in the context of improved chemotherapy, in the present study we attempted to identify novel NADPH-dependent oxido-reductases from *T. cruzi*. An aldo-keto reductase (AKR) from *T. cruzi* (*Tc*AKR) was partially purified, cloned and characterized for the first time. We show that *Tc*AKR is mainly localized in the cytosol and is able to reduce not only commonly used AKR substrates but also NQ drugs, suggesting it may be involved in trypanocidal drug metabolism.

2. Materials and methods

2.1. Parasites

Epimastigotes of *T. cruzi* CL Brener clone were cultured at 28 °C in biphasic medium containing 3% nutritive agar (Difco), with the addition of 2% rabbit defibrinated blood and 3.7% of Brain Heart Infusion (Difco). Parasites were collected after culture for 7 days. For Western Blot assays, trypomastigotes and amastigotes were obtained from infected monolayers of VERO cells.

2.2. Purification of NADPH-dependent oxido-reductases from T. cruzi epimastigotes

T. cruzi epimastigotes (1 g) suspended in 6.5 ml of 100 mM potassium phosphate pH 7, 1.15% KCl, 1 mM EDTA, 0.5 mM PMSF and 50 μg/ml TLCK were ruptured by freeze-thawing with liquid N_2. Lysates were centrifuged at 10,000 × *g* in G-Sorvall® RC-SB for 30 min at 4 °C. The soluble fraction previously filtrated through 0.8 μm nitro-cellulose filters was incubated for 1 h at room temperature with 0.2 g of Cibacron Blue-Sepharose CL-6B (Pharmacia Biotech). Bound proteins were eluted with 0.7 and 0.9 mM of NADPH. The eluted fractions were analyzed by 12% SDS-PAGE stained with Coomassie Brilliant Blue R-250 and the fractions containing proteins were dialyzed against 50 mM Tris–HCl buffer pH 8.

2.3. Identification of TcAKR by matrix assisted laser desorption/ionization time of flight mass spectrometry (MALDI-TOF-MS)

Proteins present in fractions eluted with NADPH from Cibacron Blue-Sepharose were separated by 12% SDS-PAGE, stained with Coomassie Brilliant Blue R-250 in 30% (v/v) methanol–0.5% (v/v) acetic acid and destained with 30% (v/v) methanol. A piece of gel containing the 32-kDa polypeptide was manually excised from the gel and washed twice for 30 min with 100 mM NH_4HCO_3 pH 8.3 and 50% acetonitrile (ACN) in 100 mM NH_4HCO_3 and reduced with 10 mM DTT for 1 h at 56 °C. Then iodoacetamide at a final concentration of 55 mM in 100 mM NH_4HCO_3 was added, the gel piece was incubated for 45 min at room temperature and washed for 10 min twice with 25 mM NH_4HCO_3 and 50% ACN in NH_4HCO_3 pH 8.3. The gel piece was dried under vacuum. Proteolytic in-gel digestion was performed with sequencing grade trypsin at 35 °C overnight. The peptides were extracted from gel with 60% ACN in 0.2% trifluoroacetic acid (TFA) and concentrated by vacuum centrifugation. The sample was desalted using POROS 10 R2 (Applied Biosystems, Foster City, USA) home-made microcolumns and peptides were eluted with 3 μl of matrix solution (saturated solution of α-cyano-4-hydroxycinnamic acid in 60% ACN and 0.2% TFA) and put directly into the mass spectrometer sample plate. MALDI-TOF MS measurements were carried out in a Voyager DE_PRO instrument (Applied Biosystems) equipped with a N_2 laser source (337 nm). Mass spectra were acquired in reflector mode and were internally calibrated with trypsin autolytic fragments. Proteins were identified after database searching with monoisotopic peptide masses using MASCOT search engine and including the following searching parameters: taxonomy, All entries; monoisotopic mass tolerance, 0.05 Da; partial methionine oxidation; and one missed tryptic cleavage allowed.

2.4. Cloning and sequencing of TcAKR gene

Genomic DNA was purified from *T. cruzi* epimastigotes CL Brener clone using standard procedures [13]. The following primers were used to amplify the ORF encoding *Tc*AKR: ***AKR$_{for}$*** 5′-GGGGGTACCAGAGTCATGAATTGC-3′ and ***AKR$_{rev}$*** 5′-CCGCTGCAGGTTCACTCCTCTCC-3′, containing 5′ *KpnI* site and a 3′ *PstI* site, respectively. PCR was carried out using a PCR Thermal Cycler (HYBAID Limited PCR Express HBPX220) for 35 cycles in a 25 μl reaction mixture containing 0.1 μM of primers, 1.25 U *Taq* DNA Polymerase (Promega), and 10 ng of *T. cruzi* genomic DNA under the following conditions: initial denaturation at 94 °C for 3 min, 35 cycles each with denaturation at 94 °C for 1 min, annealing at 52 °C for1 min, and extension at 72 °C for 1 min, and a final extension at 72 °C for 10 min.

A single PCR product with a length of ~900 bp was purified by Wizard® SV Gel and PCR Clean-up System (Promega), cloned into a pGEM®-T Easy vector (Promega) and sequenced using ABI Prism 377 DNA sequencer (Perkin Elmer). Protein sequence was analyzed using the Protein-BLAST algorithm (www.ncbi.nlm.nih.gov/blast) and multiple sequence alignment of *Tc*AKR with AKR family members was carried out using Clustal W 1.83 program (www.ebi.ac.uk).

*Tc*AKR gene was obtained from the recombinant vector pGEM®-T Easy-*Tc*AKR by digestion with *KpnI* and *PstI* and introduced into pQE-30 (Qiagen) excised with the same restriction enzymes.

2.5. Expression, solubility studies and purification of the recombinant TcAKR (recTcAKR) from E. coli

Escherichia coli strain M15 transformed with the recombinant plasmid pQE30-*Tc*AKR was incubated at 37 °C in Luria Broth (LB) media with shaking until the OD_{600} was 0.5–0.6. Then, expression of the rec*Tc*AKR was initiated by adding of 1 mM isopropyl-β-D-thiogalactopyranoside (IPTG). For rec*Tc*AKR solubility study, cells were grown in LB media with 660 mM D-sorbitol and 2.5 mM betaine [14]. After 3 h of growth at 37 °C, the cells were harvested, resuspended in lysis buffer (50 mM NaH_2PO_4, 300 mM NaCl, 10 mM imidazole, pH 8) and sonicated three times on ice, 10 s each, with 10 s pauses (Sonifier B-2 Brandon Sonic Power). The lysate was centrifuged at 10,000 × *g* for 30 min at 4 °C and the supernatant was loaded onto a nickel-nitrilotriacetic acid agarose column (Ni-NTA) (Qiagen) equilibrated with the same buffer. The column was washed with buffer containing 50 mM NaH_2PO_4, 300 mM NaCl and 20 mM imidazole, pH 8 until OD_{280} was stable and then the protein was eluted by adding 250 mM imidazole to the buffer. The enzyme was dialyzed overnight at 4 °C against 100 mM Tris–HCl buffer pH 7 and stored at –20 °C. Protein concentration was determined using the method of Bradford and standardized using bovine serum albu-

min (BSA). The purity of the protein was assessed by 12% SDS-PAGE and Coomassie Brilliant Blue staining.

2.6. Enzymatic assays

Reducing activity was routinely assayed by measuring NADPH oxidation spectrophotometrically at 340 nm ($\varepsilon = 6270\ M^{-1}\ cm^{-1}$) at 30 °C in a Beckman Coulter DU 640 UV. Linear rates of activity were measured over 3 min. Blanks without enzyme or substrate were included. AKR activity was determined in reaction mixtures of 0.25 ml containing an appropriate amount of enzyme in 100 mM Tris–HCl buffer pH 6.5 with either 1 mM 4-nitrobenzaldehyde (4-NBA) and 0.1 mM NADPH or 50 mM 2-dihydroxyacetone (2-DHA) and 0.2 mM NADPH. Quinone oxido-reductase (QOR) activity was evaluated spectrophotometrically with the following *o*-NQ: 9,10-phenanthrenquinone (9,10-PQ), 1,2-naphthoquinone (1,2-NQ) and β-lapachone and *p*-NQ: 5-hydroxy-1,4-naphthoquinone (5H-1,4-NQ), 2-hydroxy-1,4-naphthoquinone (2H-1,4-NQ), α-lapachone and menadione. The standard reaction mixture contained, in a final volume of 0.1 ml, 90 mM triethanolamine buffer pH 7.7, 0.1 mM NADPH, 0.025 mM quinone, 0.002 mM EDTA and an appropriate amount of enzyme. Apparent K_m or $S_{0.5}$ values were determined by measuring the initial reaction rate tested in triplicates over the following range of substrate or cofactor concentrations: 0.15–1.75 mM 4-NBA, 5–150 mM 2-DHA, 10–200 μM NADPH (AKR activity), 3–30 μM 1,2-NQ, 5–35 μM 9,10-PQ and 30–150 μM NADPH (QOR activity). Results were analyzed with the GraphPad Prism version 3.00 for Windows and GraphPad Software (San Diego California USA).

2.7. Molecular mass of recTcAKR

Purified rec*Tc*AKR was analyzed by gel chromatography on Superose 12 10/30 GL (Amersham Biosciences) column equilibrated with 150 mM Tris–HCl, pH 7.6, containing 300 mM NaCl in an AKTA purifier HPLC system (Amersham Pharmacia Biotech). Elution was performed with the same buffer at a flow rate of 0.5 ml/min at room temperature. Fractions of 0.2 ml were collected, and each fraction was analyzed by 12% SDS-PAGE and by ELISA using an anti-rec*Tc*AKR serum. Enzymatic activity of the fractions was assayed with 4-NBA, 9,10-PQ and 1,2-NQ. The molecular mass markers (Bio-Rad) used were: thyroglobulin (670 kDa), IgG (158 kDa), ovalbumin (44 kDa), myoglobin (17 kDa) and vitamin B_{12} (1.35 kDa).

Molecular mass of rec*Tc*AKR was also evaluated by mass spectrometer. In that case proteins were analyzed in a LCQ Duo, (ESI-IT) mass spectrometer from ThermoFisher (San Jose, CA, USA). Proteins were loaded through a 250 μl syringe, at 12.5 μl/min, in a 28 μl/min flow coming from a Surveyor pump. Solvent used was methanol: water: acetic acid (50:50:2). The mass spectrometer operated in full scan mode, between 400 and 2000 *m*/*z*.

2.7.1. Measurement of superoxide

Generation of superoxide was determined by measuring superoxide dismutase (SOD)-inhibitable reduction of acetylated cytochrome C at 550 nm ($\varepsilon = 21{,}000\ M^{-1}\ cm^{-1}$) according to Kumagai et al. [15]. The reaction mixture contained (final volume: 0.1 ml) 80 mM Tris–HCl buffer pH 7.7, 0.1 mM NADPH, 0.002 mM EDTA, 0.025 mM acetylated cytochrome c, the quinone (0.025 mM 9,10-PQ or 0.010 mM 1,2-NQ) and rec*Tc*AKR (9 μg or 0.3 μg for 9,10-PQ and 1,2-NQ reactions, respectively) in the absence or presence of SOD (100 U).

2.7.2. Electron spin resonance (ESR) measurements

The presence of 5,5′-dimethyl-1-pyrroline N-oxide (DMPO) adducts was studied under aerobic conditions in a reaction mixture containing 0.025 mM quinone (9,10-PQ or β-lapachone), 0.1 mM NADPH, 100 mM DMPO, 0.002 mM EDTA, 80 mM Tris–HCl buffer pH 7.7 and an appropriate amount of enzyme. Spectrometer setting is indicated in the figure legend.

Semiquinone radical detection was performed under anaerobiosis in a reaction mixture containing 0.0025 and 0.8 mM quinone (9,10-PQ or β-lapachone), 0.1 and 1.6 mM NADPH, 0.002 mM EDTA, 80 mM Tris–HCl buffer pH 7.7 and 15 μg of rec*Tc*AKR. In order to obtain anaerobic conditions for the ESR measurements, the assay media (less quinones) were bubbled with a stream of nitrogen for 5 min. At the same time, the quinone solution was bubbled with nitrogen, as above. A sample of the deoxygenated, concentrated quinone solution was added to the deoxygenated assay medium and the mixture was further bubbled with nitrogen for 1 min. Lastly, the reaction medium was transferred to the spectrometer cell previously flushed with nitrogen, the head space of the cell was flushed with nitrogen and the spectrum was recorded. The time elapsed from the reaction mixture preparation to ESR spectra recording was about 20 min, a period which is considered as the incubation time. ESR measurements were performed at room temperature using a Bruker ECS 106 ESR spectrometer (Bruker, Karlsruhe, Germany) equipped with a ER 4102 ST cavity. Spectrometer setting was: microwave power, 40 mW; microwave frequency, 9,42 GHz; modulation amplitude, 1 G; modulation frequency, 50 kHz; time constant, 328 ms; and conversion time, 82 ms. The field was centered at 3490 G and the swept width was 50 G.

2.8. Preparation of a mouse recTcAKR-specific antiserum and Western Blot analysis

Four-week-old male BALB/c mice were immunized subcutaneously with five weekly doses of 50 μg of rec*Tc*AKR in 100 mM Tris–HCl buffer pH 6.5 with incomplete Freund's adjuvant. Seven days after the last immunization the animals were bled and the serum used for western blot analysis. For doing that, the corresponding samples were boiled 3 min in SDS-PAGE sample buffer and analyzed by 12% SDS-PAGE followed by electroblotting onto nitro-cellulose membranes. Blots were blocked with 5% skimmed milk in PBS and incubated for 1 h at room temperature and 30 min at 37 °C with mouse anti-rec*Tc*AKR polyclonal antibodies in the dilution indicated in the legend of the respective figure. Membrane was washed with PBS and then incubated for 1 h at room temperature with biotinylated anti-mouse IgG (Jackson) diluted 1:2000. After washes, membranes were incubated with streptavidin-horseradish peroxidase (Jackson) diluted 1:1000 for 30 min at room temperature. Detection was performed with ECL™ Western Blotting Analysis System (Amersham).

2.9. Blue Native polyacrylamide gel electrophoresis (BN-PAGE)

To separate total parasite lysates by BN-PAGE, 10^7 epimastigotes were lysed by freezing and thawing in 50 μl of 15% glycerol, 50 mM Bis–Tris–HCl, pH 7.0. BN-PAGE (4–20%) were prepared and run at 4 °C as described [16] using the Mini Protean III system from Bio-Rad. Western blotting was done as described in section 5.9. The water soluble proteins used for molecular mass calibration of BN-PAGE were: ferritin, dimeric and monomeric forms (880 and 440 kDa); albumin, dimeric and monomeric forms (132 and 66 kDa) and chymotrypsinogen (25 kDa).

2.10. ELISA assay for detection of TcAKR

Besides the measurement of its activity, the amounts of *Tc*AKR present in different enzymatic fractions obtained as indicated in the text were also evaluated by ELISA. Briefly, flat-bottomed plates were coated overnight at 4 °C with the antigens and afterward blocked with 5% skimmed milk in PBS. After being

washed with PBS-0.05%-tween20 (PBS-T), plates were incubated for 1 h at room temperature with mouse anti-rec*Tc*AKR polyclonal antibodies diluted 1:500. After washing, plates were incubated for 1 h at room temperature with anti-mouse IgG-horseradish peroxidase (Jackson) diluted 1:2000. Color was developed with *o*-phenylenediamine dihydrochloride (OPD) and optical density was read at 490 nm.

2.11. Partial permeabilization by digitonin treatment

The experiment was performed as described previously [17]. *T. cruzi* epimastigotes (125 mg wet weight) were used for each digitonin concentration analyzed. The activities of the cytosolic marker pyruvate kinase, the glycosomal marker hexokinase, the Golgi marker acid phosphatase and the mitochondrion marker citrate synthase were determined in all fractions. The extraction percentage of *Tc*AKR in all fractions was evaluated by ELISA immunoassay.

3. Results

3.1. Purification of NADPH-dependent oxido-reductases from T. cruzi and TcAKR identification

It is widely known that Cibacron Blue F3 is capable of binding adenylyl-containing substances [18]. In an attempt to obtain NADPH-dependent oxido-reductases from *T. cruzi*, soluble fraction of epimastigote lysates was incubated with Cibacron Blue-Sepharose and bound proteins were eluted with 0.7 or 0.9 mM

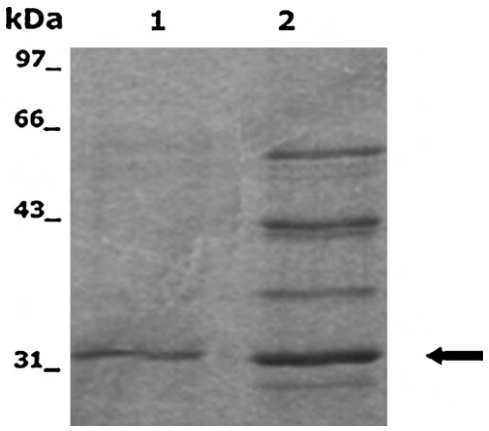

Fig. 1. Purification of NADPH-dependent oxido-reductases from *T. cruzi*. 12% SDS-PAGE of fractions eluted from Cibacron Blue-Sepharose and stained with Coomassie Brillant Blue R-250. Elution was performed with 0.7 mM (lane 1) and 0.9 mM (lane 2) NADPH. Arrow indicates the main 32 kDa polypeptide eluted with NADPH and selected for further characterization.

```
TcAKR                    ----MNCNYSCVTLHNSAQMPQLGLGVWRAQDGAETANAVRWAIEAGYRH  46
T. brucei PGFs           ----MALTQS-LKLSNGVMMPVLGFGMWKLQDGNEAETATMWAIKSGYRH  45
B. cereus 2,5 DKGR       ----MHIPTT--TLHNGVKMPMIGLGVYKAKEGDEVKQAVKTALEVGYRS  44
S. cerevisiae GCY1P      MPATLHDSTKILSLNTGAQIPQIGLGTWQSKE-NDAYKAVLTALKDGYRH  49
                             :    .  .* ... :* :*:* :: ::  :.  *.  *:: ***

TcAKR                    IDTAYFYNNEKGVGQGIRESGVPREEVWVTTKVWNSDLGYEKTLAAFERS  96
T. brucei PGFs           IDTAAIYKNEESAGRAIASCGVPREELFVTTKLWNSDQGYESTLSAFEKS  95
B. cereus 2,5 DKGR       IDTATVYENESGVGEAIRESGIPREDIFITTKVWNDDQGYEETLEAFEKS  94
S. cerevisiae GCY1P      IDTAAIYRNEDQVGQAIKDSGVPREEIFVTTKLWCTQ--HHEPEVALDQS  97
                         **** .*.**. .*..* ..*:***:::***:*  :  :...  *:::*

TcAKR                    RELLGLEYIDLYLIHWPGKKK--------------------------F 118
T. brucei PGFs           IKKLGLEYVDLYLIHWPGKDK--------------------------F 117
B. cereus 2,5 DKGR       LKKLQMDYVDLYLIHWPVRGK--------------------------Y 116
S. cerevisiae GCY1P      LKRLGLDYVDLYLMHWPARLDPAYIKNEDILSVPTKKDGSRAVDITNWNF 147
                          : * ::*:****:*** : .                          :

TcAKR                    VDTWKALEKLYEEKKVRAIGVSNFEPHHLTELFKS--CKIPPLVNQVELH 166
T. brucei PGFs           IDTWKAFEKLYADKKVRAIGVSNFHEHHIEELLKH--CKVAPMVNQIELH 165
B. cereus 2,5 DKGR       VDTYRALEKLYEEGKVRAIGVSNFHKHHLELLLPN--CKVKPMVNQVELH 164
S. cerevisiae GCY1P      IKTWELMQELPKTGKTKAVGVSNFSINNLKDLLASQGNKLTPAANQVEIH 197
                         :.*:. :::*    *.:*:*****  :::  *:     *: * .**:*:*

TcAKR                    PLFQQRALREFCKQHNIAVTAWSPLGSGDRTGFLKNHVLGEIAKKHNKSP 216
T. brucei PGFs           PLLNQKALCEYCKSKNIAVTAWSPLGQG---HLVEDARLKAIGGKYGKTA 212
B. cereus 2,5 DKGR       PMLTQFELRNYCQDEQIQMEAWSPLMRGG--EVFQHPIIQAIANKYEKTP 212
S. cerevisiae GCY1P      PLLPQDELINFCKSKGIVVEAYSPLGSTD-APLLKEPVILEIAKKNNVQP 246
                         *:: *  * ::*:.. * : *:***       ..:.  :  *. *    .

TcAKR                    AQVVIRWDIQHGIVTIPKSTNKGRIQENFNVWDFKLTEEEMRQIDELNED 266
T. brucei PGFs           AQVMLRWEIQAGVITIPKSGNEARIKENGNIFDFELTAEDIQVIDGMNAG 262
B. cereus 2,5 DKGR       AQVILRWDIQSGIVTIPKSVTPSRIKENFTIFDFALTEEEIRQINTLNRD 262
S. cerevisiae GCY1P      GHVVISWHVQRGYVVLPKSVNPDRIKTNRKIFT--LSTEDFEAINNISKE 294
                         .:*:: *.:* * :.:*** .  **: * .::   *: *::. *: :.

TcAKR                    KRFGGHPDNFFPGGEE-- 282
T. brucei PGFs           HRYGPDPEVFMNDF---- 276
B. cereus 2,5 DKGR       LHVGTNPDKYDTL----- 275
S. cerevisiae GCY1P      KGEKRVVHPNWSPFEVFK 312
                                  .
```

Fig. 2. Multiple sequence alignment of the *Tc*AKR amino-acid sequence with members of the AKR super-family. *Tc*AKR sequence (accession no. EU558869) is aligned with: *T. brucei* PGFS, prostaglandin $F_{2\alpha}$ synthase (accession no. BAB17681); *B. cereus* 2,5 DKGR, 2,5-diketo-D-gluconic acid reductase (accession no. NP_833815) and *S. cerevisiae* GCY1P, glycerol dehydrogenase (accession no. NP_01476). Tryptic peptides from *Tc*AKR which matched to a putative PGFS from *T. cruzi* GeneDB database (accession no.Tc00.1047053511287.49) are boxed and shadowed in *Tc*AKR sequence. Strictly conserved residues in the primary structure of all AKRs are shadowed and the strictly conserved residues of the AKR cofactor-binding pocket are boxed. * indicates identical amino acids. : and · indicate conserved and semi-conserved amino-acid substitutions, respectively.

Table 1
Kinetic parameters of rec*Tc*AKR.

Substrate	V_{max} (μmol NADPH/min/mg)	K_m or $S_{0.5}$ (mM)	n (Hill coefficient)	V_{max}/K_m
AKR activity				
4-NBA	0.66 ± 0.04	0.67 ± 0.13	1.2	0.98
2-DHA	0.14 ± 0.001	27.50 ± 0.57	1.0	0.005
$NADPH_{4\text{-NBA}}$	0.49 ± 0.07	0.04 ± 0.002	1.2	13.19
$NADPH_{2\text{-DHA}}$	0.05 ± 0.01	0.02 ± 0.01	1.2	2.27
NADH[a]	Not detected	–	–	–
QOR activity				
1,2-NQ	5.30 ± 1.41	0.01 ± 0.004[b]	2.2	588.89
9,10-PQ	0.12 ± 0.002	0.02 ± 0.002[b]	2.0	6.55
NADPH	0.04 ± 0.002	0.05 ± 0.004[b]	2.3	0.75

[a] 0.1 mM of NADH and 1 mM of 4-NBA (rec*Tc*AKR between 1.5 and 6 μg) or 0.1 mM of NADH and 50 mM of DHA (rec*Tc*AKR between 5 and 60 μg).
[b] For enzymes with sigmoid kinetics, when Hill coefficient value is far from 1, $S_{0.5}$ was calculated from Hill equation.

NADPH. SDS-PAGE analysis of the resultant affinity chromatography fractions eluted with 0.7 mM NADPH demonstrated the presence of a single 32-kDa polypeptide. However, when the purification fractions eluted with 0.9 mM NADPH were analyzed, besides the major 32-kDa polypeptide, four polypeptides of mass 57.5, 45, 37.2 and 29.1 kDa were also visible (Fig. 1).

Since the 32-kDa polypeptide was the main component of the 0.7 mM NADPH-eluted fraction and its apparent molecular weight did not coincide with previously described NADPH-dependent oxido-reductases from *T. cruzi*, we proceeded to identify this protein by MALDI-TOF after in-gel tryptic digestion. The peptide-mass spectrum obtained was submitted to the *T. cruzi* sequencing genome project database [19]. The data query returned that ten of twenty-two mass values of the spectrum matched with a putative prostaglandin F synthase (PGFS) of 32.775 kDa (GeneDB_Tcruzi: Tc00.1047053511287.49) with a MASCOT significant score of 122 and a sequence coverage of 38% (Fig. 2). Since the 32-kDa polypeptide purified by affinity chromatography with Cibacron Blue F3 and NADPH elution was identified as a *T. cruzi* non-characterized member of the AKR super-family, it was denominated *Tc*AKR.

3.2. Cloning and expression of recombinant TcAKR

In order to obtain the *TcAKR* gene, 3′- and 5′-primers were designed taking as template the sequence from GeneDB_Tc database (accession number Tc00.1047053511287.49) which aligned with the tryptic peptides produced by the digestion of the 32 kDa polypeptide. The full *TcAKR* open reading frame (900 bp) was amplified by PCR from *T. cruzi* CL Brener genomic DNA, cloned in pGemT Easy vector and sequenced. A database search and alignment of the *Tc*AKR amino-acid sequence revealed that it has 41–59% of similarity to proteins belonging to the AKR super-family from a variety of organisms, namely PGFS from *T. brucei* (59%), 2,5-diketo-D-gluconic acid reductase (2.5 DKGR) from *B. cereus* (58%) and glycerol dehydrogenase (GCY1) from *Saccharomyces cerevisiae* (41%). Moreover, the *Tc*AKR sequence presented all key amino-acid

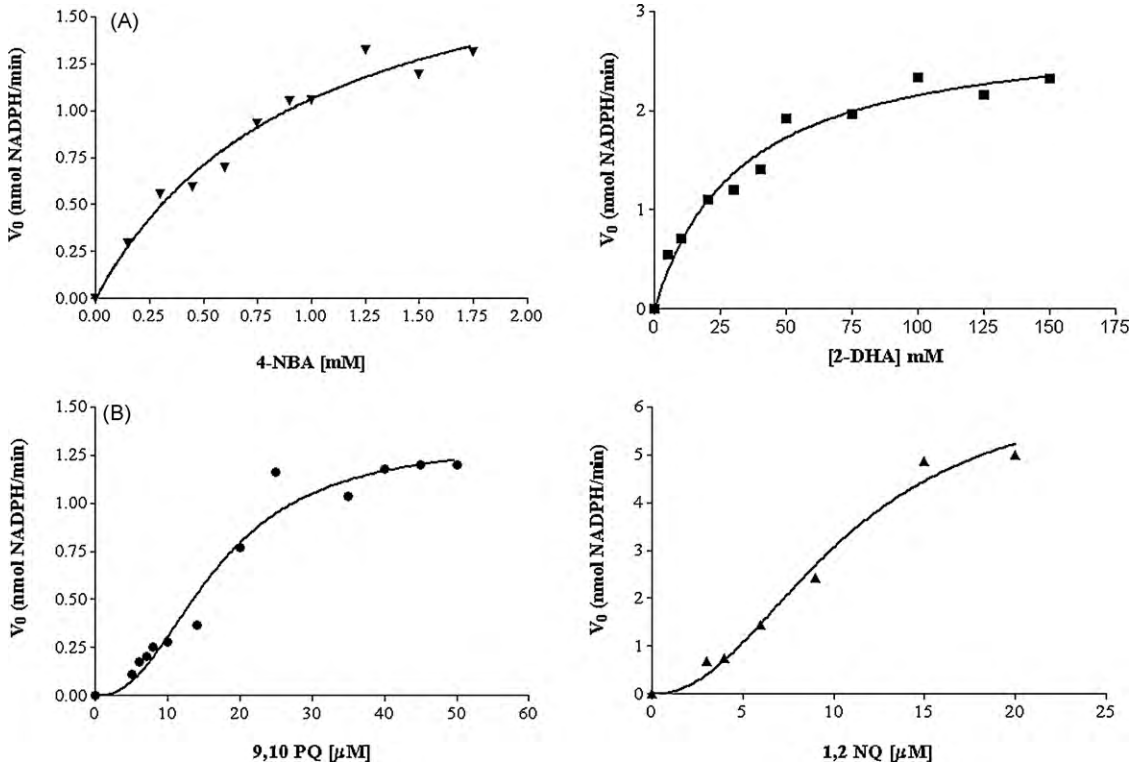

Fig. 3. Substrate saturation curve for AKR activity and QOR activity by *recTc*AKR. Initial velocity was assayed in triplicate by measuring the absorbance at 340 nm. The curves drawn are the best-fit curves calculated by the Hill equation using the GaphPad Prism program. (A) Michaelis–Menten curves for 4-NBA and 2-DHA as substrate, with 3 μg and 20 μg respectively of *recTc*AKR, used under the conditions described in Section 2. (B) Sigmoidal curves for 9,10-PQ and 1,2-NQ as substrates, with 12 μg and 6 μg respectively of *recTc*AKR, used under the conditions described in Section 2.

Table 2
QOR activity of rec*Tc*AKR from *T. cruzi*.

Substrate (25 μM)	Activity (μmol NADPH/min/mg enzyme)	Relative activity (%)
1,2-NQ	42.10 ± 3.39	100
9,10-PQ	0.63 ± 0.04	1.50
β-Lapachone	0.28 ± 0.02	0.67
α-Lapachone	0	–
5H-1,4-NQ (Juglone)	0	–
2H-1.4-NQ	0	–
Menadione	0	–

residues conserved in all members of the AKR super-family [20–22] (Fig. 2).

The *TcAKR* gene was subcloned in pQE30 and expressed in *E. coli* M15 strain after IPTG induction. Upon SDS-PAGE, the rec*Tc*AKR exhibited the expected molecular mass of 32 kDa (Fig. S1, lane 2), however, most of the recombinant protein proved to be insoluble (Fig. S1, lanes 3 and 4). Since it has been previously described that D-sorbitol and betaine favor the solubilization of foreign proteins expressed in *E. coli* [14], recombinant *E. coli* was cultured in the presence of these reagents. In this way, a greater proportion of rec*Tc*AKR was in the soluble fraction of the lysates (Fig. S1, lanes 5 and 6). rec*Tc*AKR was purified from this fraction by Ni-NTA column in native conditions obtaining a yield of 26 mg/l of culture (Fig. S1, lane 7).

3.3. Biochemical characterization of recTcAKR

To determine whether rec*Tc*AKR has catalytic activity towards aldehydes and ketones, two common AKR substrates, 4-NBA and 2-DHA, were evaluated as substrates of this enzyme. It showed to be active with both substrates using NADPH as a cofactor. No activity was detected with NADH as a cofactor under the conditions tested (Table 1). Maximum activity was observed at pH 6.5 irrespective of the substrate used (Fig. S2). With both substrates, plots of reaction velocity versus substrate concentration showed a classical hyperbola (Fig. 3A) consistent with a Michaelis–Menten behavior. K_m and V_m values for 4-NBA, 2-DHA and NADPH estimated from Lineweaver–Burk plots showed that rec*Tc*AKR acts more efficiently with 4-NBA than with 2-DHA (Table 1). Plots of reaction velocity versus NADPH concentration, for both substrates, showed also a classical hyperbola (data not shown).

Reductase activity with 4-NBA and 2-DHA using NADPH as a cofactor was also evaluated with the native enzyme purified from epimastigotes by Cibacron Blue affinity chromatography as described above. Activities in these fractions were proportional to the amount of protein present with specific activities of 0.43 and 0.14 μmol of NADPH/min/mg of protein for 4-NBA and 2-DHA, respectively.

Since it has been previously described that NADPH-dependent reductases from *T. cruzi* contribute to the metabolism of antitrypanosomal drugs [23,24,12,3], we tested the hypothesis that *Tc*AKR may reduce quinones. rec*Tc*AKR showed a QOR activity with *o*-NQ (1,2-NQ, 9,10-PQ and β-lapachone), but it did not show activity with *p*-NQ, such as 5H-1,4-NQ, 2H-1,4-NQ, α-lapachone and menadione (Table 2). The substrate saturation curve with *o*-NQ fit to a sigmoidal curve (Fig. 3B) significantly better than to a rectangular hyperbola ($p < 0.05$). As the sigmoidal rate plot can be described by the Hill equation, the $S_{0.5}$ (equivalent to the K_m parameter for Michaelis–Menten kinetics) was calculated for these substrates. In both cases, the value of Hill coefficient (n) was approximately 2 (Table 1), suggesting that rec*Tc*AKR presents a cooperative behavior [25]. Conversely, a calculated Hill coefficient of 1 for 4-NBA and 2-DHA is consistent with a Michaelis–Menten behavior. Results from

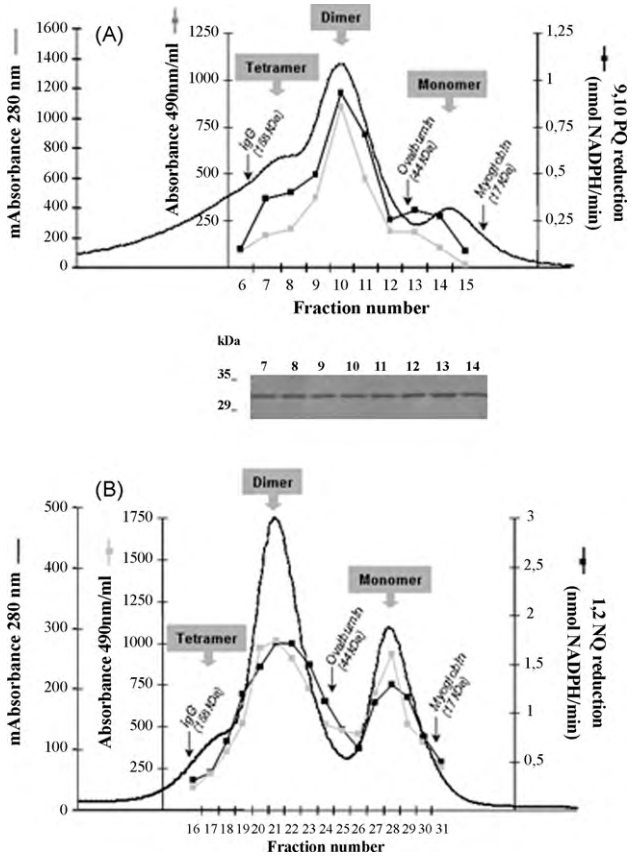

Fig. 4. Gel filtration and SDS-PAGE pattern of *recTc*AKR. Protein elution was recorded as $OD_{280\,nm}$. Putative monomeric, dimeric and tetrameric peaks are indicated. *recTc*AKR was identified, in all fractions, by ELISA with an anti-*recTc*AKR represented by arbitrary units of $OD_{490\,nm}$/ml (□) and by enzymatic activity (■) (nmol NADPH/min) using 9,10-PQ (A) and 1,2-NQ (B) as substrates. 12% SDS-PAGE of Superose 12 fractions (A) showed a single band of 32 kDa for all the fractions. Arrows indicate molecular weight standards of gel filtration: IgG, ovalbumin and myoglobin.

kinetic experiments summarized in Table 1 reveal that 1,2-NQ is the best substrate among the quinones tested for rec*Tc*AKR. When NADPH was the variable substrate, plots of velocity versus NADPH concentration showed also sigmoidal kinetics for QOR activity (data not show).

3.4. Molecular mass of recTcAKR

Since sigmoidal kinetics is associated to oligomeric enzymes, rec*Tc*AKR was submitted to gel filtration experiments on a Superose 12 column in order to asses its quaternary structure. rec*Tc*AKR eluted from the gel filtration column in three peaks corresponding to molecular masses of 31.2, 69.2 and 118.2 kDa which were assigned to monomers, dimers and tetramers, respectively. rec*Tc*AKR was found to be preponderantly dimeric. However, we observed that the proportion between monomer and tetramer varied in different preparations (Fig. 4A and B). Detection of rec*Tc*AKR by ELISA in the eluted fractions showed the same distribution as protein elution (Fig. 4A and B). Moreover, rec*Tc*AKR elution correlated with AKR activity using 4-NBA (data not shown) and QOR activity with 9,10-PQ (Fig. 4A) or 1,2-NQ (Fig. 4B) as substrates indicating that all the fractions presented enzymatic activity. Monomeric (fractions 12–14), dimeric (fractions 9–12) and tetrameric (fractions 7–9) fractions showed a single band of 32 kDa in SDS-PAGE consistent with the presence of homodimers and homotetramers of rec*Tc*AKR (Fig. 4A).

Table 3
Superoxide anion production by rec*Tc*AKR during QOR activity.

Substrate (25 μM)	NADPH consumption (μmol/mim/ml)	Superoxide anion generation SOD-inhibitable (μmol/mim/ml)	$\frac{O_2^-\text{ production}}{\text{NADPH consumption}}$
9,10-PQ	0.10 ± 0.01	0.21 ± 0.04	2.0
1,2-NQ	12.45 ± 0.78	19.45 ± 1.77	1.6

These results were confirmed by mass spectrometry. Fractions corresponding to the dimeric and monomeric forms of the enzyme were submitted to mass spectrometry analysis as indicated under Section 2. Both spectra presented similar envelopes showing m/z signals between 750 and 1600 (Fig. S3A). The deconvoluted molecular weight for the monomeric form was 34,754 Da and for the dimeric form showed to be around 69,000–74,000 Da with very low resolution (Fig. S3B). The last one is compatible with a dimeric structure.

In order to evaluate the oligomeric state of the native *Tc*AKR, epimastigote proteins were separated under native conditions by BN-PAGE and analyzed by western blot using an anti-rec*Tc*AKR serum. Two major bands corresponding to molecular masses of 33 and 74 kDa, respectively were obtained which are compatible with the monomeric and dimeric forms of the enzyme (Fig. S4).

3.5. Production of free radicals

When either 9,10-PQ or 1,2-NQ was incubated with rec*Tc*AKR in the presence of an excess amount of NADPH at 30 °C for 2 min, superoxide anion formation was detected by reduction of acetylated cytochrome C as described in Section 2. In the presence of SOD (100 U), the reduction of cytochrome C was decreased by 70% and 66%, respectively. Simultaneously, NADPH consumption was measured and a calculated ratio of SOD-inhibitable superoxide anion generation and NADPH consumption of approximately 2:1 was obtained for both substrates. These results are indicated in Table 3.

Spin trapping experiments were carried out in the presence of DMPO. After 14 accumulated scans, a small but clear 1:2:2:1 quartet spectrum was detected when the complete reaction mixture was assayed, both with β-lapachone and with 9,10-PQ as substrates (Fig. 5A and B). Based on the hyperfine splittings ($a^N = a^H = 14.9$ G), signals were assigned to hydroxyl radical-DMPO [26,27]. In the same incubation conditions used for kinetic experiments, but under anaerobiosis the ESR signals for the semiquinone radicals of 9,10-PQ and β-lapachone were not detected. However, when higher concentrations of quinones and NADPH (0.8 mM and 1.6 mM, respectively) were used, multiline ESR spectra identified as the 9,10-PQ or β-lapachone semiquinone radical metabolite were observed even in the absence of enzyme, suggesting that under the latter condition, the quinones and the cofactor can react non-enzymatically (data not shown).

3.6. Expression of TcAKR in different developmental stages of T. cruzi and subcellular localization

Polyclonal antibodies raised against rec*Tc*AKR reacted with a 32-kDa protein in epimastigote lysates by western blot assays (Fig. 6, lane 2). Anti-rec*Tc*AKR also recognized the main 32-kDa polypeptide in epimastigote fractions eluted with NADPH from Cibacron Blue-Sepharose (Fig. 6, lane 1), confirming this protein is indeed the *Tc*AKR. Western blot analysis of amastigote and trypomastigote lysates demonstrated *Tc*AKR is also expressed in *T. cruzi* stages present in mammalian host (Fig. 6, lane 3 and lane 4, respectively).

With the aim to study the subcellular localization of *Tc*AKR a progressive permeabilization of epimastigotes was performed by increasing amounts of digitonin, as indicated in Section 2. Thereafter, the liberation of several enzymatic marker activities was followed. Upon increasing the relative concentration of digitonin the first enzyme liberated was the cytosolic marker pyruvate kinase. The release of *Tc*AKR was followed by ELISA using the mouse anti-rec*Tc*AKR serum and showed to be similar to pyruvate kinase release profile, suggesting *Tc*AKR is localized in cytosol (Fig. 7).

4. Discussion

We report here the identification, cloning and biochemical characterization of the *Tc*AKR, a novel NADPH-dependent

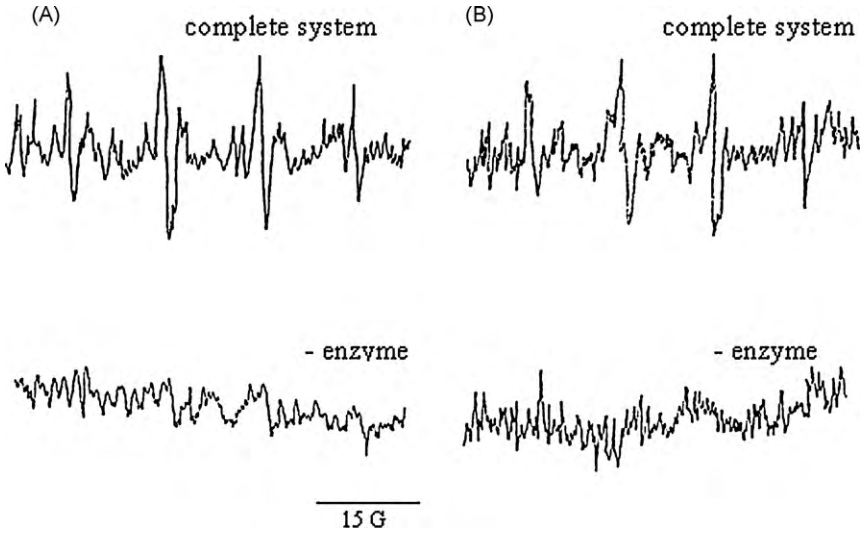

Fig. 5. ESR spectra of DMPO-adducts produced by using β-lapachone (A) or 9-10-PQ (B) as substrate in the absence or the presence of the enzyme. Incubation mixture containing 0.0025 mM quinone (β-lapachone or 9,10-PQ), 0.1 mM NADPH, 0.002 mM EDTA, 80 mM Tris–HCl buffer pH 7.7 and 15 μg of rec*Tc*AKR was measured by ESR at room temperature. Spectrometer setting was: microwave power, 20 mW; microwave frequency, 9,75 GHz; modulation amplitude, 0,5G; modulation frequency, 50 kHz; time constant, 655 ms; and conversion time, 164 ms. The field was centered at 3480 G and the swept with was 100 G.

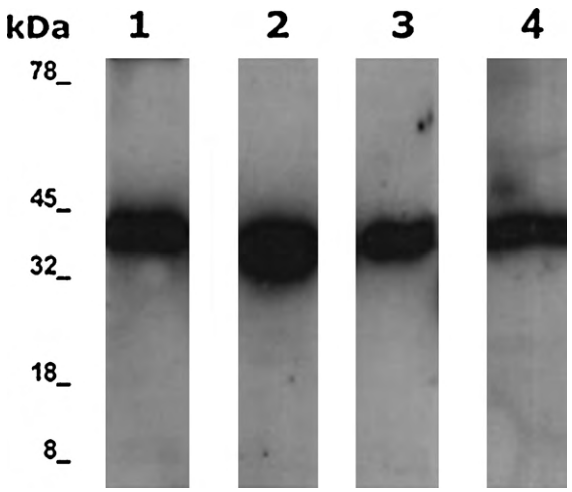

Fig. 6. Western blot analysis of *Tc*AKR in cell extracts from different stages of *T. cruzi*. After blotting, membranes containing: lane 1, *Tc*AKR eluted with 0.7 mM NADPH from Cibacron Blue-Sepharose; lane 2, 1.8×10^6 epimastigote lysates; lane 3, 9×10^6 amastigote lysates, and lane 4, 1.8×10^7 trypomastigote lysates were assayed with anti-rec*Tc*AKR polyclonal antibodies in a dilution of 1:1000.

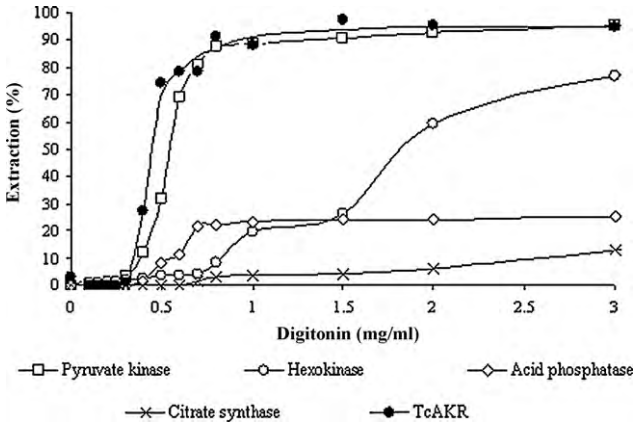

Fig. 7. Differential release of *Tc*AKR and various marker enzymes from intact *Trypanosoma cruzi* epimastigotes by titration with digitonin. Markers used are: pyruvate kinase, citosol; hexokinase, glycosomes; acid phosphatase, Golgi; citrato synthase, mitochondrion. The release of *Tc*AKR was followed by ELISA using a mouse anti-rec*Tc*AKR serum.

oxido-reductase from *T. cruzi* and the first member of the AKR super-family described in this parasite. In addition, we show evidence that this enzyme may participate in the mechanisms of action of trypanocidal drugs such as *o*-NQ with the subsequent generation of free radicals.

The capability of *Tc*AKR to reduce 4-NBA and 2-DHA with similar kinetic parameters to those reported for other AKR members [28,29] demonstrated that, besides sequence homology, this enzyme has a catalytic activity compatible with this super-family of proteins. However, its physiological role in the parasite remains to be elucidated.

The *Tc*AKR amino-acid sequence shows the highest percentage of similarity with the PGFS from *Trypanosoma brucei*, an enzyme characterized by Kubata and collaborators [24]. In a subsequent report [12], with the aim to characterize the PGFS from *T. cruzi*, these authors cloned a sequence (GenBank acc. no. AF262056) corresponding to the *Tc*AKR gene described here but lacking the 3′ end bases which codify for an 8-amino-acids C-terminal extension. As they failed to express this recombinant protein they concluded, in contrast with our results, that the AKR gene was non-functional in *T. cruzi*. They proved instead that the enzyme responsible for

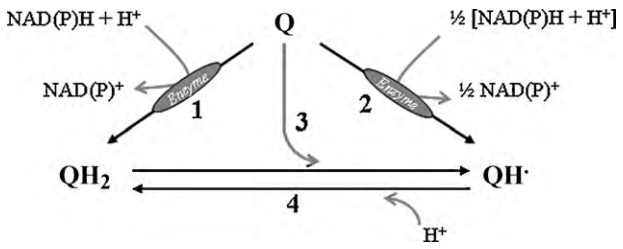

Fig. 8. Pathway of quinone metabolism. Two-electron reduction of quinone (arrow 1); one-electron reduction of quinone (arrow 2); disproportionation reaction through interaction hydroquinone with quinone (arrow 3) and conversion of accumulated semiquinone radical to hydroquinone (arrow 4).

prostaglandin $F_{2\alpha}$ synthesis in *T. cruzi* is the flavoenzyme *Tc*OYE [12]. In this regard, it is worthwhile mentioning that we could not detect NADPH reduction when prostaglandin H_2 was used as substrate for rec*Tc*AKR, which suggests that this enzyme may not be involved in prostaglandin synthesis (data not shown).

The use of 2-DHA as substrate and its similarity to a glycerol dehydrogenase from *S. cerevisiae* allow us to hypothesize that *Tc*AKR may fulfill a related function in *T. cruzi*. It is worthwhile mentioning that the enzymes involved in the glycerol pathway have not been characterized so far in this parasite. The fact that *T. cruzi* epimastigotes are able to grow in the presence of glycerol as substitute of glucose as carbon source (Cannata JJB, unpublished results) and the presence of a putative DHA kinase sequence in the predicted proteins database from TSK-TSC [19] raise the possibility that glycerol catabolism in *T. cruzi* could proceed via DHA as it has been described in yeast [30].

Currently available chemotherapy for Chagas' disease, based on the nitrofuran nifurtimox or the nitroimidazole benznidazole, is effective for acute infections, but it presents both limited efficacy in the prevalent chronic stage of the disease as well as frequent toxic side effects [2]. In this context, efforts have been addressed to find new prototype compounds among natural and synthetic sources. Quinones are important naturally occurring pigments widely distributed in nature which are associated with anticancer, antibacterial, antimalarial, and fungicide activities [31]. Many natural and synthetic NQ, such as menadione, lapachol and β-lapachona display notable trypanocidal activities [32–36]. It has been proposed that the molecular basis of quinone toxicity is the production of ROS after their intra-cellular reduction. These compounds are enzymically reduced via two different pathways: (i) hydroquinones (QH_2) are formed by a two-electron reduction pathway (Fig. 8, arrow 1) and (ii) semiquinone radicals ($QH^{\bullet}$) are formed via one-electron reduction pathway (Fig. 8, arrow 2). QH_2 is capable of interacting with the quinone (Q) through a disproportionation reaction to yield the semiquinone radical (Fig. 8, arrow 3) [37]. In addition, accumulated $QH^{\bullet}$ may convert to QH_2 (Fig. 8, arrow 4) [38]. Semiquinone radicals react with molecular oxygen, resulting in the generation of superoxide anions and QH_2 forms redox cycling with both molecular oxygen and superoxide [37]. In this regard, cumulative evidence has shown that redox cycling of NQ is present in trypanosomatids and several of these compounds act as subversive substrates of *T. cruzi* flavoenzymes [39,11,12,3]. Our results suggest that not only flavoenzymes are involved in the mechanisms of action of trypanocidal drugs, since rec*Tc*AKR showed NADPH-dependent reductase activity with *o*-NQ drugs such as β-lapachone, 9,10-PQ and 1,2-NQ, with concomitant generation of free radicals. Although we cannot conclude from our data if quinone reduction by *Tc*AKR is carried out through one- or two-electron reduction pathways, ROS production was evidenced by the following facts: (1) *Tc*AKR reduction of 9,10-PQ and 1,2-NQ lead to formation of superoxide anion with the expected stoichiometric ratio of superoxide anion production and NADPH consumption (2:1) [40] and (2)

ESR experiments revealed that hydroxyl radical was formed after reduction of 9,10-PQ and β-lapachone; this DMPO-OH signal can arise either from the breakdown of the superoxide adduct of DMPO (DMPO-OOH) (not detectable by ESR under our experimental conditions), and/or the direct trapping of the hydroxyl radical [41]. These observations may be explained by the following chemical reactions:

$$QH^{\bullet} + O_2 \rightarrow Q + O_2^{\bullet -} + H^+ \quad (5)$$

$$QH_2 + O_2 \rightarrow Q + H_2O_2 + H^+ \quad (6)$$

$$O_2^{\bullet -} + O_2^{\bullet -} + 2H^+ \rightarrow H_2O_2 + O_2 \quad (7)$$

$$H_2O_2 + O_2^{\bullet -} \rightarrow HO^{\bullet} + H_2 + HO^- \quad (8)$$

The semiquinone radical, generated either by one-electron reduction of the quinone or through the reaction of QH_2 with the quinone, reacts with molecular oxygen producing superoxide anion ($O_2^{\bullet}$) [reaction (5)]. Hydrogen peroxide (H_2O_2) is generated by either oxidation of hydroquinone by molecular oxygen [reaction (6)] or disproportion of superoxide anion [reactions (7)]. Finally, hydroxyl radical ($HO^{\bullet}$) is generated from H_2O_2 and superoxide by the Haber-Weiss reaction [reaction (8)] [33,37,38]. The lack of the detection of semiquinone radicals in our system suggests either these species may be unstable intermediates or that in anaerobiosis, conversion of $QH^{\bullet}$ to QH_2 would be the predominant reaction (Fig. 8, arrow 4), while in aerobiosis the $QH^{\bullet}$ is auto-oxidized to superoxide anion [reaction (5)].

Contrary to *Tc*OYE, which can catalyze reduction of either *o*- or *p*-NQ [12], *Tc*AKR was not able to reduce any of the *p*-NQ tested in this study, 2H-1,4-NQ, 5H-1,4-NQ, α-lapachone and menadione. Thus, we can conclude *Tc*AKR is specific for *o*-NQ. *Tc*OYE has been postulated as one of the major enzymes used by *T. cruzi* to catalyze redox cycling of NQ, but nevertheless Kubata and col. also mention the presence of β-lapachone reductases other than *Tc*OYE in accordance with our results [12]. Otherwise, the presence of NQ reductase activity in mitochondrial and microsomal fractions of epimastigotes indicates that other unidentified enzymes from *T. cruzi* are also involved in drug metabolism [33,35].

Although AKRs so far studied are most commonly monomeric, multimeric forms have been described [42]. Here we demonstrate that rec*Tc*AKR is present in three oligomeric forms, namely monomer, homodimer and homotetramer, the dimer being the preponderant one. Monomeric and dimeric forms were also detected in epimastigote lysates confirming that dimerization occurs *in vivo* and is not solely an artifact of the recombinant protein. The lack of tetrameric forms of *Tc*AKR in the lysates may indicate that these complexes are either not formed *in vivo* or their concentration is too low to be detected under the experimental conditions used. Mass spectrometry analysis of the rec*Tc*AKR dimeric form yielded a mass compatible with a dimeric structure, which was striking because under the experimental conditions prevailing during that procedure, oligomeric proteins are usually dissociated into its monomers. This fact suggests that the interactions among the subunits are strong enough to maintain the oligomeric structure during mass spectrometry conditions without preventing spontaneous dissociation when it is in solution. Usually, activity of enzymes that can exist in different oligomeric forms is associated exclusively to one of the forms. In our case, we observed activity with all the fractions obtained by gel filtration corresponding to the three oligomeric forms. However, this does not necessarily mean that the three forms are equally active because they can be in a dynamic equilibrium.

The sigmoidal kinetics obtained when *Tc*AKR is assayed with *o*-NQ substrates is consistent with positive cooperativity [25] and with the oligomeric nature of this enzyme as well. Positive cooperativity has also been reported for other AKRs as the human liver cytosolic AKR [43] and other detoxifying enzymes [44,45]. On the other hand, when 4-NBA and 2-DHA were used as substrates for *Tc*AKR, the typical hyperbolic type behavior was observed. Mutational analysis suggested that quinone reduction occurs via mechanisms that differ from physiological substrate reduction [46]. Moreover, crystal structure and site-directed mutagenesis of *Trypanosoma brucei* PGFS, the most homologous protein to *Tc*AKR, demonstrate that different amino-acid residues are required for the reduction of 9,10-PQ and the biological reduction of prostaglandin H_2 to prostaglandin $F_{2\alpha}$ [47]. Future crystallographic studies of *Tc*AKR in the presence of quinones or AKR substrates will elucidate the catalytic mechanisms used by this enzyme in each case.

Acknowledgments

This work was supported by the Instituto Nacional de Parasitología "Dr. Mario Fatala Chaben" - A.N.L.I.S. "Dr. Carlos G. Malbrán", the NASA/ChagaSpace network and Universidad de Buenos Aires (UBA). AMR and MG are members of the Research Career of the National Research Council of Argentina (CONICET). We are grateful to Dr. Susana Linskens (Laboratorio Nacional de Investigación y Servicio en Péptidos y Proteínas [LANAIS-PRO], Facultad de Farmacia y Bioquímica, UBA) for her support on ESI mass spectrometry.

Appendix A. Supplementary data

Supplementary data associated with this article can be found, in the online version, at doi:10.1016/j.molbiopara.2010.05.019.

References

[1] Nakajima-Shimada J, Hirota Y, Aoki T. Inhibition of *Trypanosoma cruzi* growth in mammalian cells by purine and pyrimidine analogs. Antimicrob Agents Chemother 1996;40:2455–8.
[2] Urbina JA, Docampo R. Specific chemotherapy of Chagas disease: controversies and advances. Trends Parasitol 2003;19:495–501.
[3] Uchiyama N, Kabututu Z, Kubata BK, et al. Antichagasic activity of komaroviquinone is due to generation of reactive oxygen species catalyzed by *Trypanosoma cruzi* old yellow enzyme. Antimicrob Agents Chemother 2005;49:5123–6.
[4] Fairlamb AH, Cerami A. Metabolism and functions of trypanothione in the Kinetoplastida. Annu Rev Microbiol 1992;46:695–729.
[5] Nogoceke E, Gommel DU, Kiess M, Kalisz HM, Flohe L. A unique cascade of oxidoreductases catalyses trypanothione-mediated peroxide metabolism *in Crithidia fasciculata*. Biol Chem 1997;378:827–36.
[6] Wilkinson SR, Meyer DJ, Kelly JM. Biochemical characterization of a trypanosome enzyme with glutathione-dependent peroxidase activity. Biochem J 2000;352(Pt 3):755–61.
[7] Wilkinson SR, Meyer DJ, Taylor MC, Bromley EV, Miles MA, Kelly JM. The *Trypanosoma cruzi* enzyme TcGPXI is a glycosomal peroxidase and can be linked to trypanothione reduction by glutathione or tryparedoxin. J Biol Chem 2002;277:17062–71.
[8] Viode C, Bettache N, Cenas N, et al. Enzymatic reduction studies of nitroheterocycles. Biochem Pharmacol 1999;57:549–57.
[9] Maya JD, Bollo S, Nunez-Vergara LJ, et al. *Trypanosoma cruzi*: effect and mode of action of nitroimidazole and nitrofuran derivatives. Biochem Pharmacol 2003;65:999–1006.
[10] Blumenstiel K, Schoneck R, Yardley V, Croft SL, Krauth-Siegel RL. Nitrofuran drugs as common subversive substrates of *Trypanosoma cruzi* lipoamide dehydrogenase and trypanothione reductase. Biochem Pharmacol 1999;58:1791–9.
[11] Salmon-Chemin L, Buisine E, Yardley V, et al. 2- and 3-substituted 1,4-naphthoquinone derivatives as subversive substrates of trypanothione reductase and lipoamide dehydrogenase from *Trypanosoma cruzi*: synthesis and correlation between redox cycling activities and in vitro cytotoxicity. J Med Chem 2001;44:548–65.
[12] Kubata BK, Kabututu Z, Nozaki T, et al. A key role for old yellow enzyme in the metabolism of drugs by *Trypanosoma cruzi*. J Exp Med 2002;196:1241–51.
[13] Sambrook J, Fritsch EF, Maniatis T. Molecular cloning: a laboratory manual. 2nd ed. Cold Spring Harbor: Cold Spring Harbor Laboratory Press; 1989.
[14] Blackwell JR, Horgan R. A novel strategy for production of a highly expressed recombinant protein in an active form. FEBS Lett 1991;295:10–2.
[15] Kumagai Y, Koide S, Taguchi K, et al. Oxidation of proximal protein sulfhydryls by phenanthraquinone, a component of diesel exhaust particles. Chem Res Toxicol 2002;15:483–549.

[16] Schägger H, Cramer WA, von Jagow G. Analysis of molecular masses and oligomeric states of protein complexes by blue native electrophoresis and isolation of membrane protein complexes by two-dimensional native electrophoresis. Anal Biochem 1994;217(2):220–30.
[17] Maugeri D, Cazzulo JJ. The pentose phosphate pathway in *Trypanosoma cruzi*. FEMS Microbiol Lett 2004;234:117–23.
[18] Easterday RL, Easterday IM. Affinity chromatography of kinases and dehydrogenases on Sephadex and Sepharose dye derivatives. Adv Exp Med Biol 1974;42:123–33.
[19] El-Sayed NM, Myler PJ, Bartholomeu DC, et al. The genome sequence of *Trypanosoma cruzi*, etiologic agent of Chagas disease. Science 2005;309:409–15.
[20] Jez JM, Bennett MJ, Schlegel BP, Lewis M, Penning TM. Comparative anatomy of the aldo-keto reductase superfamily. Biochem J 1997;326(Pt 3):625–36.
[21] Jez JM, Penning TM. The aldo-keto reductase (AKR) superfamily: an update. Chem Biol Interact 2001;130–132:499–525.
[22] Ellis EM. Microbial aldo-keto reductases. FEMS Microbiol Lett 2002;216:123–31.
[23] Henderson GB, Ulrich P, Fairlamb AH, et al. "Subversive" substrates for the enzyme trypanothione disulfide reductase: alternative approach to chemotherapy of Chagas disease. Proc Natl Acad Sci U S A 1988;85:5374–8.
[24] Kubata BK, Duszenko M, Kabututu Z, et al. Identification of a novel prostaglandin f (2alpha) synthase in *Trypanosoma brucei*. J Exp Med 2000;192:1327–38.
[25] Houston JB, Kenworthy KE. In vitro-in vivo scaling of CYP kinetic data not consistent with the classical Michaelis–Menten model. Drug Metab Dispos 2000;28:246–54.
[26] Kumagai Y, Arimoto T, Shinyashiki M, et al. Generation of reactive oxygen species during interaction of diesel exhaust particle components with NADPH-cytochrome P450 reductase and involvement of the bioactivation in the DNA damage. Free Radic Biol Med 1997;22(3):479–87.
[27] Zweier JL, Duke SS, Kuppusamy P, Sylvester JT, Gabrielson EW. Electron paramagnetic resonance evidence that cellular oxygen toxicity is caused by the generation of superoxide and hydroxyl free radicals. Febs Lett 1989;252(1–2):12–6.
[28] Petrash JM, Murthy BS, Young M, et al. Functional genomic studies of aldo-keto reductases. Chem Biol Interact 2001;130–132:673–83.
[29] Miller JV, Estell DA, Lazarus RA. Purification and characterization of 2,5-diketo-D-gluconate reductase from *Corynebacterium sp*. J Biol Chem 1987;262:9016–20.
[30] Norbeck J, Blomberg A. Metabolic and regulatory changes associated with growth of *Saccharomyces cerevisiae* in 1.4 M NaCl. Evidence for osmotic induction of glycerol dissimilation via the dihydroxyacetone pathway. J Biol Chem 1997;272:5544–54.
[31] Koyama J. Anti-infective quinone derivatives of recent patents. Recent Pat Anti-infect Drug Discov 2006;1:113–25.
[32] Docampo R, Lopes JN, Cruz FS, Souza W. *Trypanosoma cruzi*: ultrastructural and metabolic alterations of epimastigotes by beta-lapachone. Exp Parasitol 1977;42:142–9.
[33] Boveris A, Docampo R, Turrens JF, Stoppani AO. Effect of beta-lapachone on superoxide anion and hydrogen peroxide production in *Trypanosoma cruzi*. Biochem J 1978;175:431–9.
[34] Goijman SG, Stoppani AO. Effects of beta-lapachone, a peroxide-generating quinone, on macromolecule synthesis and degradation in *Trypanosoma cruzi*. Arch Biochem Biophys 1985;240:273–80.
[35] Menna-Barreto RF, Henriques-Pons A, Pinto AV, Morgado-Diaz JA, Soares MJ, De Castro SL. Effect of a beta-lapachone derived naphthoimidazole on *Trypanosoma cruzi*: identification of target organelles. J Antimicrob Chemother 2005;56:1034–41.
[36] Salas C, Tapia RA, Ciudad K, et al. *Trypanosoma cruzi*: activities of lapachol and alpha- and beta-lapachone derivatives against epimastigote and trypomastigote forms. Bioorg Med Chem 2008;16:668–74.
[37] Taguchi K, Fujii S, Yamano S, et al. An approach to evaluate two-electron reduction of 9,10-phenanthraquinone and redox activity of the hydroquinone associated with oxidative stress. Free Radic Biol Med 2007;43:789–99.
[38] Maruyama A, Kumagai Y, Morikawa K, Taguchi K, Hayashi H, Ohta T. Oxidative-stress-inducible *qor*A encodes an NADPH-dependent quinone oxidoreductase catalysing a one-electron reduction in *Staphylococcus aureus*. Microbiology 2003;149:389–98.
[39] Molina Portela MP, Fernandez Villamil SH, Perissinotti LJ, Stoppani AO. Redox cycling of o-naphthoquinones in trypanosomatids. Superoxide and hydrogen peroxide production. Biochem Pharmacol 1996;52:1875–82.
[40] Rao PV, Krishna CM, Zigler JS. Identification and characterization of thew enzymatic activity of Z-crystallin from guinea pig lens. J Biol Chem 1992;267:96–102.
[41] Buettner GR. Spin trapping: ESR parameters of spin adducts. Free Radic Biol Med 1987;3:259–303.
[42] Hyndman D, Bauman DR, Heredia VV, Penning TM. The aldo-keto reductase superfamily homepage. Chem Biol Interact 2003;143–144:621–31.
[43] Rosemond MJ, St John-Williams L, Yamaguchi T, Fujishita T, Walsh JS. Enzymology of a carbonyl reduction clearance pathway for the HIV integrase inhibitor, S-1360: role of human liver cytosolic aldo-keto reductases. Chem Biol Interact 2004;147:129–39.
[44] Korzekwa KR, Krishnamachary N, Shou M, et al. Evaluation of atypical cytochrome P450 kinetics with two-substrate models: evidence that multiple substrates can simultaneously bind to cytochrome P450 active sites. Biochemistry 1998;37:4137–47.
[45] Witherow LE, Houston JB. Sigmoidal kinetics of CYP3A substrates: an approach for scaling dextromethorphan metabolism in hepatic microsomes and isolated hepatocytes to predict in vivo clearance in rat. J Pharmacol Exp Ther 1999;290:58–65.
[46] Schlegel BP, Ratnam K, Penning TM. Retention of NADPH-linked quinone reductase activity in an aldo-keto reductase following mutation of the catalytic tyrosine. Biochemistry 1998;37:11003–11.
[47] Kilunga KB, Inoue T, Okano Y, et al. Structural and mutational analysis of *Trypanosoma brucei* prostaglandin H2 reductase provides insight into the catalytic mechanism of aldo-keto reductases. J Biol Chem 2005;280:26371–82.